Tuning of Record-Based Stochastic Ground Motion Models for Hazard-Compatibility and Applications to Seismic Risk Assessment

Christopher R. Vetter
Ph.D. Candidate, Dept. of Civil & Environmental Engineering & Earth Sciences, University of Notre Dame, Notre Dame, IN, USA

Alexandros A. Taflanidis
Associate Professor, Dept. of Civil & Environmental Engineering & Earth Sciences, University of Notre Dame, Notre Dame, IN, USA

George P. Mavroeidis
Assistant Professor, Dept. of Civil & Environmental Engineering & Earth Sciences, University of Notre Dame, Notre Dame, IN, USA

ABSTRACT: This paper discusses the tuning of stochastic ground motion models so that compatibility of the resultant hazard with Ground Motion Prediction Equations (GMPEs) is directly established. This is facilitated by proper optimization for the predictive relationships involved in such models that relate seismicity characteristics to the model parameters. A computationally efficient approach is discussed that can seamlessly provide ground motions that match any chosen GMPE for any desired set of seismicity characteristics or structural periods. Foundation of the methodology is the development of a metamodel that facilitates a simplified relationship between the ground motion model parameters and its median predictions. This metamodel is subsequently used to efficiently select the predictive relationships that optimize the match to the chosen GMPE with the numerical accuracy of the metamodel predictions also explicitly incorporated in this optimization. The implementation of the tuned model within seismic risk assessment is also demonstrated.

1. INTRODUCTION

Stochastic ground motion models facilitate a versatile description of earthquake acceleration time histories by modulating a stochastic sequence through functions that address spectral and temporal properties of the excitation (Papadimitriou 1990; Boore 2003; Rezaeian and Der Kiureghian 2010). This is established by relating the parameters of these functions to earthquake (such as rupture distance and moment magnitude) and site (such as shear wave velocity) characteristics through appropriate predictive relationships. Various frameworks have been proposed for developing such ground motion models, namely distinguishing between the approaches adopted for establishing the predictive relationships they involve. Source-based models (Boore 2003) rely on physical modeling of the rupture and wave propagation mechanisms, whereas record-based models (Papadimitriou 1990; Rezaeian and Der Kiureghian 2010) are developed by fitting a preselected "waveform" to a suite of recorded ground motions. The validation of these models is frequently performed (Boore 2003; Rezaeian and Der Kiureghian 2010) by comparison of their predictions to the ones from Ground Motion Prediction Equations (GMPEs). As GMPEs represent the established approach for developing seismic hazard maps (Petersen et al. 2008), compatibility of the seismic risk (acceleration time-histories) provided by ground motion models to GMPEs is a desired property.

This has provided a motivation to look at the explicit selection of the predictive equations of stochastic ground motion models to establish a

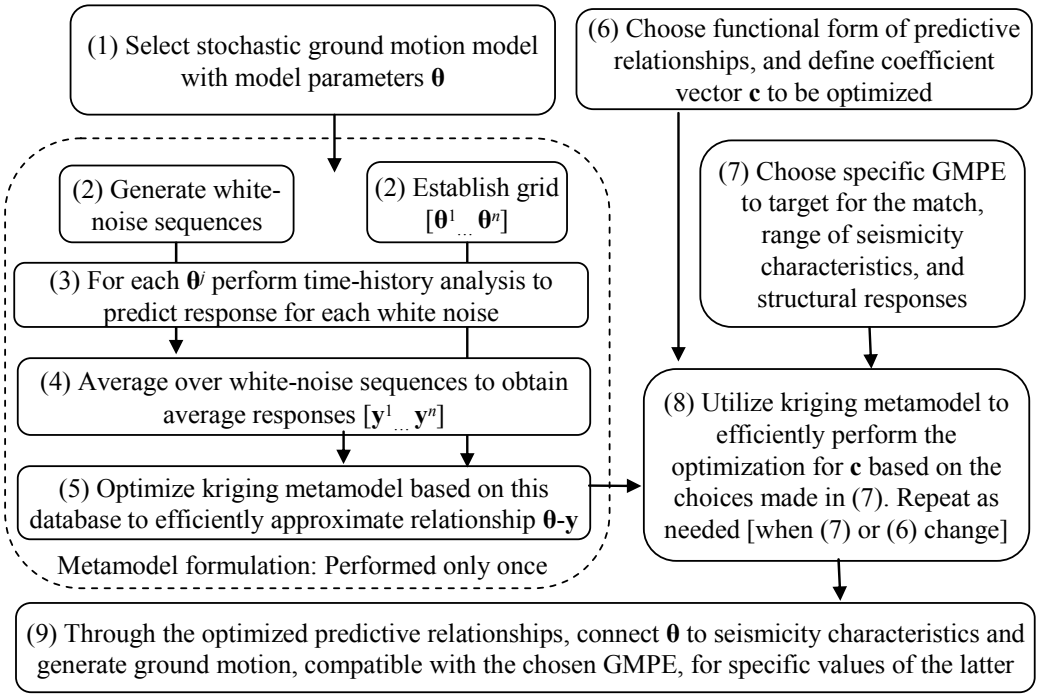

Figure 1. Schematic of the proposed implementation for GMPE compatible ground motion modeling.

match of the resultant median risk to the spectral acceleration estimates of GMPEs (Scherbaum et al. 2006). The study by Scherbaum et al. (2006) though, focused on a match to a specific, elastic GMPE and a preselected range of seismicity characteristics and structural periods of interest, whereas its reliance on an optimization framework based on genetic algorithms creates some computational constraints pertaining to the number of characteristics related to the predictive equations that can be optimized. The present study revisits this problem of developing GMPE-compatible stochastic ground motion models, but rather than targeting a-priori a specific GMPE it offers a versatile and computationally efficient framework utilizing surrogate modeling concepts. The framework is demonstrated using the record-based model proposed recently by Rezaeian and Der Kiureghian (2010) with some of the modifications initially suggested by Papadimitriou (1990). The tuning of this model to different GMPEs is first established and subsequently the implementation of the tuned models for the assessment of seismic risk is considered while a comparison to risk described through scaling of motions is also presented.

2. GMPE-COMPATIBLE GROUND MOTION MODELING FRAMEWORK

An overview of the proposed framework is provided in Figure 1. To formalize this process consider a stochastic ground motion model that provides acceleration time histories $\ddot{a}(t\,|\,\boldsymbol{\theta},\mathbf{W})$ by modulating a white-noise sequence, $\mathbf{W}$, through appropriate time/frequency functions that are parameterized through the n_θ-dimensional *model parameter* vector $\boldsymbol{\theta}\in\mathbb{R}^{n_\theta}$. This vector defines the model and is typically composed of various excitation properties such as Arias intensity, strong ground motion duration or parameters related to frequency characteristics of the ground motion. Section 3 presents the specific model chosen for this study. We are interested here in choosing the predictive equations that relate $\boldsymbol{\theta}$ to seismicity and local site properties such as moment magnitude, M, rupture distance, r_{rup}, or shear wave velocity in the upper 30 meters, V_{s30}. Let $\mathbf{z}$ denote the vector of such properties, referenced herein as *seismological parameters*. For each model parameter θ_i these relationships will involve unknown coefficients $c_{il}; l=1,..,n_{ic}$ with $\mathbf{c}\in\mathbb{R}^{n_c}$, denoting the unknown *coefficient vector*. We will represent by $\boldsymbol{\theta}=\mathbf{G}(\mathbf{z}\,|\,\mathbf{c})$ these n_θ relationships.

The objective is to ultimately select the coefficient vector $\mathbf{c}$ to match GMPE predictions. This compatibility can look at different response quantities of interest, including both (i) characteristics of the ground motion, such as Peak Ground Acceleration (PGA), Velocity (PGV) and Displacement (PGD), or (ii) elastic spectral responses for different periods of a single-degree-of-freedom (SDOF) elastic or inelastic oscillator (Boore and Atkinson 2008; Power et al. 2008). It is established by considering the match to a range of *seismicity scenarios*. To formalize this idea, let $\{\mathbf{z}^k; k=1,...,n_s\}$ denote the set of n_s scenarios considered, $Y_i(\mathbf{z})$ the relationship provided by the GMPEs for each response quantity and $\overline{Y}_i(\mathbf{z}\,|\,\mathbf{c})$ the median predictions provided through the stochastic ground motion model. These predictions are ultimately a function of only the model parameters $\boldsymbol{\theta}$, $\overline{Y}_i(\boldsymbol{\theta}) = \overline{Y}_i(\mathbf{G}(\mathbf{z}\,|\,\mathbf{c}))$.

The GMPE compatibility is enforced then by adopting as an objective function the average weighted square error

$$f_{opt} = \frac{1}{n_z n_y} \sum_{k=1}^{n_z} \sum_{i=1}^{n_y} \gamma_{ki}^2 \left(Y_i(\mathbf{z}^k) - \overline{Y}_i(\mathbf{z}^k\,|\,\mathbf{c}) \right)^2 \quad (1)$$

where γ_{kj} correspond to the weights penalizing the different error components (further discussed in Section 6). The optimal vector $\mathbf{c}$ is then obtained by the nonlinear, constrained optimization problem

$$\begin{aligned} \mathbf{c}^* &= \arg\min_c f_{opt} \\ \text{given } \mathbf{c}_{\min} \le \mathbf{c} \le \mathbf{c}_{\max};\ & \mathbf{b}_l \le \mathbf{f}_c(\mathbf{c}) \le \mathbf{b}_u \end{aligned} \quad (2)$$

where $\mathbf{c}_{min}$ and $\mathbf{c}_{max}$ define the lower and upper thresholds for the box bounded region for $\mathbf{c}$, and $\mathbf{f}_c(\mathbf{c})$ represents the vector of nonlinear constraints with upper and lower bounds b_l and b_u, respectively. Since the optimization problem in Eq. (2) is expected to be non-convex, the box-bounded constraints restrict appropriately the search space allowing for a global optimization approach to be adopted for its solutions, while additionally guaranteeing any desired trends in the predictive equations. The second set of (functional) constraints in Eq. (2) can be further utilized to enforce physical restrictions for the model parameters so that their values fall within specific ranges for different seismicity characteristics. This can be used to guarantee that the resultant ground motions comply with any regional trends and their parameters have physically meaningful values.

Moving finally to performing the optimization in Eq. (1), rather than targeting a-priori specific characteristics (response quantities, GMPEs, ranges for $\mathbf{z}$ or functional forms for the predictive equations), a versatile optimization framework is considered here utilizing surrogate modeling. Foundation of the formulation is the fact that the predictions from the ground motion model are ultimately functions of only $\boldsymbol{\theta}$. Thus the metamodel needs to be simply developed to approximate relationship $\overline{Y}_i(\boldsymbol{\theta})$, considering every potential response quantity of interest, without being concerned about the specific parameters defining $\mathbf{z}$ or the exact form of relationships $\boldsymbol{\theta} = \mathbf{G}(\mathbf{z}\,|\,\mathbf{c})$. This metamodel provides a highly efficient approximation to the input-output relationship $\boldsymbol{\theta} - \overline{Y}_i(\boldsymbol{\theta})$ and is established by first developing a large database $\{\boldsymbol{\theta}^j - \overline{Y}_i(\boldsymbol{\theta}^j); j=1,...,n\}$ for a properly selected grid of *support points* $\{\boldsymbol{\theta}^j; j=1,...,n\}$ and then using this information to tune the characteristics of the metamodel. A kriging metamodel will be considered here for this purpose since it has a proven capability to approximate highly complex functions (Lophaven 2002), while simultaneously providing gradient information and allowing to explicitly consider the metamodel approximation error within the optimization formulation. The stochastic ground motion model that is utilized for the illustrative implementation in this paper is reviewed next.

3. GROUND MOTION MODEL

The particular stochastic ground motion model chosen for this study is a record-based model which addresses efficiently both temporal and spectral non-stationarities (Papadimitriou 1990; Rezaeian and Der Kiureghian 2010). The former is established through a time-domain modulating envelope function while the latter is achieved by filtering a white-noise process by a filter

corresponding to multiple cascading SDOF oscillators with time-varying characteristics. The discretized time history of the ground motion can be expressed according to this model as (Rezaeian and Der Kiureghian 2010)

$$\ddot{a}(t \mid \boldsymbol{\theta}, \mathbf{W}) = q(t, \boldsymbol{\theta}) \sum_{i=1}^{k} \frac{h[t - t_i, \boldsymbol{\theta}(t_i))] w(i\Delta t)}{\sqrt{\sum_{j=1}^{k} h[t - t_j, \boldsymbol{\theta}(t_j))]^2}} \qquad (3)$$

$$k\Delta t < t < (k+1)\Delta t$$

where $\mathbf{W} = [w(i\Delta t) : i = 1, 2, ..., N_T]$ is the Guassian white-noise sequence, Δt is the chosen discretization interval, $q(t, \boldsymbol{\theta})$ is the time-modulating function, and $h[t - \tau, \boldsymbol{\theta}(\tau)]$ is an impulse response function corresponding to the pseudo-acceleration response of a linear SDOF oscillator with time varying frequency $\omega_f(\tau)$ and damping ratio $\zeta_f(\tau)$, in which τ denotes the time of the pulse

$$h[t - \tau, \boldsymbol{\theta}(\tau))] = \frac{\omega_f(\tau)}{\sqrt{1 - \zeta_f^2(\tau)}} \exp\left[-\omega_f(\tau)\zeta_f(\tau)(t - \tau)\right]$$
$$\times \sin\left[\omega_f(\tau)\sqrt{1 - \zeta_f^2(\tau)}(t - \tau)\right]; \quad \tau \le t \qquad (4)$$
$$= 0; \quad \text{otherwise}$$

For the time varying characteristics, the functions proposed in (Papadimitriou 1990) are adopted

$$\omega_f(\tau) = \omega_r + (\omega_p - \omega_r)\left(\frac{\omega_s - \omega_r}{\omega_p - \omega_r}\right)^{\tau / t_{\max}}$$
$$\zeta_f(\tau) = \alpha_f(\tau) / \omega_f(\tau) \qquad (5)$$
$$\alpha_f(\tau) = \omega_p \zeta_p + (\omega_r \zeta_r - \omega_p \zeta_p)\tau / t_{dur}$$

With ω_p, ω_s, and ω_r corresponding to the primary, secondary, and surface wave frequencies, respectively, ζ_p and ζ_r corresponding to the primary and surface wave damping, respectively, and $t_{\max}$ representing the time at which the maximum intensity of the ground motion is achieved. Parameter t_{dur} should be taken as a sufficiently large time (Papadimitriou 1990), and is chosen here to be proportional to the time that 95% of the Arias intensity is reached, t_{95}, so that $t_{dur} = \alpha_{dur} t_{95}$ with α_{dur} corresponding to an additional model parameter.

The time envelope is chosen as

$$q(t, I_a, \alpha_2, \alpha_3) = \sqrt{I_a}\left[\sqrt{\frac{2}{\pi}\frac{(2\alpha_3)^{2\alpha_2 - 1}}{\Gamma(2\alpha_2 - 1)}}\right] \qquad (6)$$
$$\times t^{\alpha_2 - 1} \exp(-\alpha_3 t)$$

where $\Gamma(.)$ is the gamma function, I_a is the Arias intensity expressed in terms of g, and $\{\alpha_2, \alpha_3\}$ are additional parameters controlling the shape and total duration of the envelope that can be related to various physical parameters. Here, the strong motion duration, D_{5-95} (defined as the duration for the Arias intensity to increase from 5% to 95% of its final value), and the peak of the envelope function, λ_p, are used. The latter is defined, based on the recommendations of (Boore 2003), as the ratio of time corresponding to the peak of the envelope to the time corresponding to 95% of its peak value. The pair $\{\alpha_2, \alpha_3\}$ can be then easily determined based on the values of $\{D_{5-95}, \lambda_p\}$ (Rezaeian and Der Kiureghian 2010).

Ultimately, the ground motion model has as parameters $\boldsymbol{\theta}$={I_a, $D_{5\text{-}95}$, λ_p, α_{dur}, ω_p, ω_s, ω_r, ζ_p, ζ_r} with the first one directly impacting (scaling) the output (thus input-output relationship is known) and the remaining eight, denoted by $\mathbf{x}$ herein, having a complex nonlinear relationship to that output. Thus $\boldsymbol{\theta} = \{I_a, \mathbf{x}\}$. For the responses that are considered in the illustrative example in this study, corresponding to linear response characteristics of SDOF responses, the aforementioned scaling of the input (ground motions) translates to a direct scaling for this output. The normalized responses will be denoted s_i herein, so that

$$\overline{Y}_i(\boldsymbol{\theta}) = \sqrt{I_a} s_i(\mathbf{x}) \qquad (7)$$

4. KRIGING METAMODEL

For providing a computational efficient approximation to the input-output relationship $\boldsymbol{\theta} - \overline{Y}_i(\boldsymbol{\theta})$ a kriging metamodeling approach is adopted. Since based on (7) the relationship to I_a is known, this pertains ultimately to the remaining parameters, $\mathbf{x}$. The kriging predictor has a Gaussian nature with mean $\overline{s}_i(\mathbf{x})$ and

standard deviation $\sigma_i(x)$ (Lophaven 2002). Each response output is approximated here through this predictor, leading to

$$s_i(\mathbf{x}) = \overline{s}_i(\mathbf{x}) + \varepsilon_i(\mathbf{x}) \tag{8}$$

where ε_i is a Gaussian zero mean approximation error with variance $\sigma_i^2(\mathbf{x})$. If $\mathbf{s}$ denotes the n_s-dimensional output vector, composed of all responses $\{s_i; i = 1,...,n_s\}$ that we want the metamodel to cover, initially a database with n observations is obtained that provides information for the $\mathbf{x} - \mathbf{s}(\mathbf{x})$ pair. For this purpose n samples for $\{\mathbf{x}^j, j = 1,...,n\}$, also known as *support points*, are created following a latin hypercube grid over the expected range of values possible for each x_i. The median predictions provided through the ground motion model are then established considering n_w white-noise samples. Using this dataset, the kriging model is then formulated. Further details for this development may be found in (Lophaven 2002). Ultimately the metamodel provides a highly efficient (within fractions of a few seconds) estimation for $\overline{s}_i$, $\sigma_i(x)$ as well as for their gradients (with respect to $\mathbf{x}$ always).

5. OPTIMIZATION OF PREDICTIVE RELATIONSHIPS

The optimization in Eq. (2) can be efficiently performed by using the kriging approximation (8). Additionally, the approximation error can be explicitly considered leading to a transformation of the objective function of Eq. (1) to

$$f_{opt} = \frac{1}{n_s n_y} \sum_{k=1}^{n_s} \sum_{i=1}^{n_y} \gamma_{ki}^2 E\left[\left(Y_i(\mathbf{z}^k) - \overline{Y}_i(\mathbf{z}^k \mid \mathbf{c})\right)^2\right] \tag{9}$$

where $E[.]$ stands for expectation under the approximation error of the kriging metamodel. Utilizing Eqs. (7) and (8), expanding the quadratic term within the expectation inside the summation, and utilizing the fact that ε_i is zero mean with variance $\sigma_i^2(\mathbf{x})$, Eq. (9) transforms to

$$f_{opt} = \frac{1}{n_z n_y} \times \sum_{k=1}^{n_z} \sum_{i=1}^{n_y} \gamma_{ki}^2 \left[\left(Y_i(\mathbf{z}^k) - \sqrt{I_a^k}\,\overline{s}_i(\mathbf{x}^k)\right)^2 + I_a^k \sigma_i^2(\mathbf{x}^k)\right] \tag{10}$$

This is the objective function that is ultimately implemented within the optimization given by Eq. (2). Estimation of this objective function is performed efficiently using the established metamodel, whereas the error of the metamodel is appropriately incorporated within. This optimization ultimately corresponds to a non-convex problem, and for finding the global minimum a two-stage numerical optimization approach is adopted in this study and implemented through the TOMLAB toolbox (Holmstrom et al. 2009). In the first stage of the optimization a direct search (gradient-free) approach is implemented to identify candidate local optima. Then in the second stage, a gradient-based optimization is performed to converge to the global optimum, using each of the previously identified candidate optima as a starting point. For improving the efficiency of the second stage, the gradient of the objective function is also analytically provided. The components of this gradient vector are

$$\frac{\partial f_{opt}}{\partial c_{il}} = \frac{1}{n_s n_y} \sum_{k=1}^{n_z} \sum_{i=1}^{n_y} \gamma_{ki}^2 \left[\left.\frac{\partial I_a \sigma_i^2(\mathbf{x})}{\partial \theta_i}\right|_{\mathbf{z}=\mathbf{z}^k} + 2\left(Y_i(\mathbf{z}^k) - \sqrt{I_a^k}\,\overline{s}_i(\mathbf{x}^k)\right) \left.\frac{\partial \sqrt{I_a}\,\overline{s}_i(\mathbf{x})}{\partial \theta_i}\right|_{\mathbf{z}=\mathbf{z}^k} \right] \left.\frac{\partial \theta_i}{\partial c_{il}}\right|_{\mathbf{z}=\mathbf{z}^k} \tag{11}$$

where the partial derivatives $\partial\theta_i / \partial c_{il}$ can easily be obtained from the established predictive relationships and the partial derivatives within the brackets are provided (analytically) directly through the kriging metamodel.

6. ILLUSTRATIVE EXAMPLE

For the illustrative implementation n=10,000 support points are used to develop the kriging metamodel. The support points are selected utilizing a latin hypercube sampling in the following ranges, [0.5s 55s] for D_{5-95}, [0.01 0.6] for λ_p, [0.7 1.5] for α_{dur}, [10 50] Hz for ω_p, [2 20] Hz for ω_s, [0.1 5] for ω_r, [0.01 0.3] for ζ_p, and [0.2 0.8] for ζ_r. The response for each support point is averaged over 400 white-noise samples to obtain the median statistics. The outputs for which the metamodel is developed

include the peak pseudo spectral acceleration of an elastic SDOF with 5% damping ratio for 22 different periods T=[0.01 0.02 0.03 0.04 0.05 0.075 0.1 0.15 0.2 0.25 0.3 0.4 0.5 0.75 1.0 1.5 2.0 3.0 4.0 5.0 7.5 10.0] s. For generating the total of 4,000,000 time histories and performing the required 92,000,000 simulations to develop the database for the metamodel close to 1000 CPU hours were required. Though this computational burden is significant, it should be stressed that it corresponds to an initial only overhead of the approach (Figure 1). Once the metamodel is developed it can be then used for any required predictions. The average (over all the outputs) absolute mean error established for the metamodel is 3%, which corresponds to very good accuracy with low computational burden, whereas each evaluation of the metamodel takes an average of 0.05 s for the entire output vector with estimation of the prediction error requiring an additional 1 s.

The seismological characteristics considered for the predictive relationships are the moment magnitude, M, and the rupture distance, r_{rup}. The compatibility is established for a specific local site condition (structure in a specific location), chosen here to $V_{s30} = 285$m/s and for a strike-slip fault. As such $\mathbf{z} = [M, r_{rup}]$. The functional forms for the predictive relationships are chosen as

$$\begin{aligned} \ln(I_a) &= c_{1,1} + c_{1,2}M + c_{1,3}\ln\sqrt{r_{rup}^{\ 2} + c_{1,5}^2} + c_{1,4}\ln(M) \\ \ln(D_{5-95}) &= c_{2,1} + c_{2,2}M + c_{2,3}\ln\sqrt{r_{rup}^{\ 2} + c_{2,4}^2} \\ \ln(\theta_j) &= c_{j,1} + c_{j,2}M + c_{j,3}r_{rup};\ j = 3,\ldots,9 \end{aligned} \tag{12}$$

with the coefficients $c_{i,l}$ $i = 1,\ldots,9$, $l = 1,\ldots,5$ formulating the coefficient vector $\mathbf{c}$ having a total of $n_c = 30$ components.

The match to the GMPE for elastic SDOF spectral acceleration proposed by (Boore and Atkinson 2008) is considered for different structural periods defining ultimately multiple outputs of interest, therefore $Y_i(\mathbf{z}) = S_{pa}(\mathbf{z}, T_i)$. The seismicity characteristics for $\mathbf{z}$ as defined as the combination of [5 6 7 8] for M and [10 30 50] km for r_{rup}, leading to n_s=12. To demonstrate the versatility of the approach two different ranges for the structural period are examined, the first (C1) corresponding to T_i chosen within a smaller range [0.3 0.4 0.5 0.75] s (therefore $n_t = 4$), and the second (C2) to a larger range [01. 0.2 0.3 0.4 0.5 0.75 1 1.5 2 3] s ($n_t = 10$).

For the optimization the weighting coefficients γ_{kj} are chosen equal to $S_{pa}(\mathbf{z}^k, T_i)$, thus establishing normalization of the output. The optimal values of the objective function are, respectively, 0.0042 and 0.0511. As expected Case 1 yields higher levels of accuracy than Case 2 (targeting a greater range of periods). The time needed to perform the optimization is 2500 s whereas if the second stage was only performed the respective requirement would have been 90 s (though guaranteeing a local only optimum). The established predictive relationships for I_a and D_{5-95} are shown in Figure 2. The results for the match are reported in Figures 3 and 4. In particular, Figure 3 reports the PSA for $S_{pa}(\mathbf{z}, T_i)$ for different M-r_{rup} and two different periods. Figure 4 shows spectral plots (for all T considered) in a similar fashion, for specific values of M and r_{rup}. In Figure 5 later an example ground motion time history is also shown.

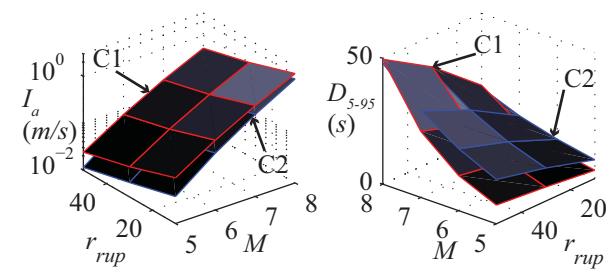

Figure 2. Optimized predictive relationships.

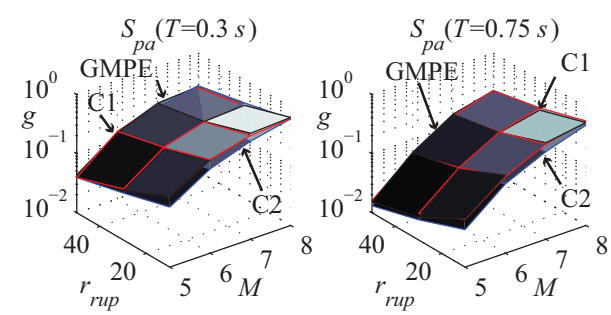

Figure 3. Comparison of GMPE predictions and tuned ground motion model predictions for different M-r_{rup} and two different periods.

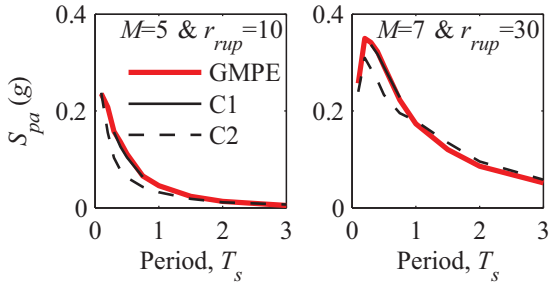

Figure 4. Spectral comparison of GMPE predictions and tuned ground motion model predictions for two different M/r_{rup} combinations

The good match to the targeted predictions is verified from the results. Case 2 (C2) encounters, as expected greater challenges. This validates the importance of targeting the specific period range of interest (rather than having a model with more general applicability) and therefore the utility of the proposed versatile framework in Figure 1 that can seamlessly support this goal.

7. SEISMIC RISK ASSESSMENT

The optimized ground motion model can be now used to support seismic risk assessment. This is demonstrated for a three-story structure (Taflanidis at al. 2013) with fundamental period T=0.505 s located within the Los Angeles basin at location 33.996°N, 118.162°W with soil characteristics V_{s30}=285m/s. The assessment follows the approach discussed in (Radu and Grigoriu 2014). Here we focus on a specific hazard level (2% probability of exceedance in 50 years) whereas the GMPE by (Boore and Atkinson 2008) is adopted to describe the regional hazard. The deaggregation (USGS, 2014) for this hazard is shown in Figure 5. The mean value for the moment magnitude and rupture distance from this deaggregation, that will be utilized within the risk assessment, are respectively $\bar{M} = 6.75$, and $\bar{r} = 8.7\,km$.

Three different approaches are adopted for characterizing acceleration time-histories for this hard. The first one (denoted R1) is based on *selection of ground motions* that for $\bar{M}$ and $\bar{r}$ match the targeted S_{pa} for the fundamental period of the structure (considered as benchmark result). The methodology proposed by Lin et, al (2013) is used for the selection, and 100 ground motions are chosen to represent the hazard (i.e. due to computational intensity of selection process a lower number is utilized here). The other two approaches use the proposed *ground motion modeling framework* with a model tuned to match S_{pa} for the fundamental period of the structure and for the range of seismic events covered in the considered deaggregation. One approach (denoted R2) considers only the mean hazard (described by $\bar{M}$ and $\bar{r}$), whereas the other (denoted R3) considers the entire range of events (different M and r_{rup}) based on the contribution P_e provided by the deaggregation. Each of these approaches utilizes 1000 ground motions with each ground motion corresponding to a different white noise input. For R2 this (i.e. white noise sequence) is the only distinction between the ground motions describing the seismic hazard.

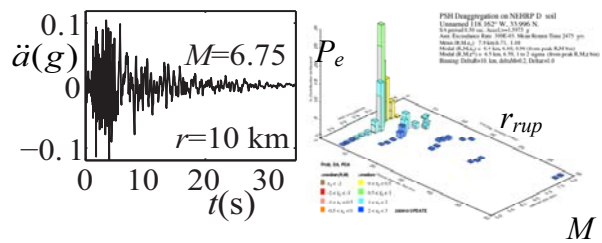

Figure 5. Example ground motion time history (left) for M=6.75, r=10km and hazard deaggregation (right) for risk assessment case study.

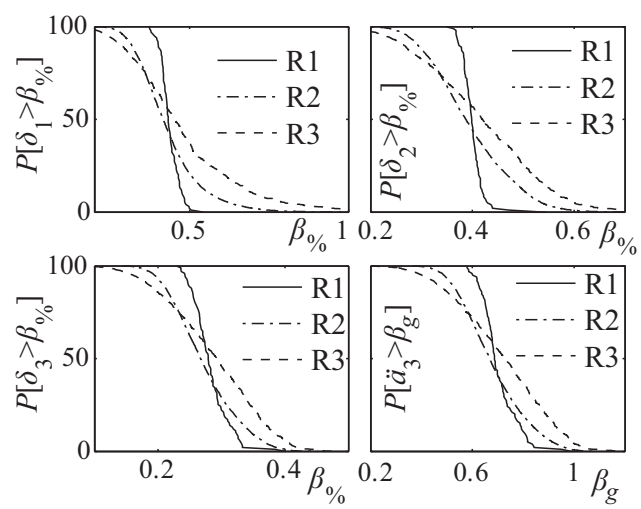

Figure 6. Probability of exceedance P[.] of different thresholds β_i for maximum inter-story drift ratio δ_i for all floors (i=1,2,3) and top floor acceleration $\ddot{a}_3$.

Figure 6 presents the probability of exceedance for different thresholds for both the drifts for all floors and absolute top-floor acceleration for all three approaches. For the median response (corresponding to 50% probability of occurrence) good agreement is observed between R2/R3 and R1 (with the latter representing the benchmark risk), while R2 and R3 provide greater variability of the response. As expected R3 has the greatest variability. For seismic risk applications this characteristic should be regarded as a desirable trait. Considering the computational efficiency for obtaining ground motions with approaches R2/R3, this demonstrates the benefits of the proposed modeling approach for seismic risk assessment applications.

8. CONCLUSIONS

The tuning of stochastic ground motion models to provide acceleration time-histories compatible with GMPEs was discussed in this paper. A framework based on kriging metamodeling was discussed to support an efficient optimization to match any desired GMPE for any chosen seismicity characteristics and structure. A model that addresses both temporal and spectral non-stationarities was selected as stochastic ground motion model in the illustrative example and the versatility of the proposed approach was verified by establishing a close match to the desired GMPEs and structural periods. The implementation of the optimized model was then considered within a seismic risk assessment application. It was shown there that the optimized model can facilitate a hazard characterization consistent with other approaches, facilitating additionally a greater variability of the resultant structural responses.

9. REFRENCES

Boore, D. M. (2003). "Simulation of ground motion using the stochastic method." *Pure Appl Geophys*, 160, 635-676.

Boore, D. M., and Atkinson, G. M. (2008). "Ground-motion prediction equations for the average horizontal component of PGA, PGV, and 5%-damped PSA at spectral periods between 0.01 s and 10.0 s." *Eartq Spectra*, 24(1), 99-138.

Holmstrom, K., Goran, A. O., and Edvall, M. M. (2009). *User's guide for TOMLAB 7*, Tomlab Optimization Inc. www.tomopt.com/tomlab/, San Diego, CA.

Lin, T., Haselton C.B., and Baker, J.W. "Conditional mean spectrum-based ground motion selection part i: hazard consistency for risk-based assessments." *Earth Eng Struct D*, 42(12), 1847-1865.

Lophaven, S. N., Nielsen, H.B., and Sondergaard, J. (2002). "DACE-A MATLAB Kriging Toolbox." Technical University of Denmark.

Papadimitriou, K. (1990). "Stochastic characterization of strong ground motion and application to structural response." *Report No. EERL 90-03*, California Institute of Technology, Pasadena, CA.

Petersen, M. D., Frankel, A. D., Harmsen, S. C., Mueller, C. S., Haller, K. M., Wheeler, R. L., Wesson, R. L., Zeng, Y., Boyd, O. S., Perkins, D. M., Luco, N., Field, E. H., Wills, C. J., and Rukstales, K. S. (2008). *Documentation for the 2008 update of the United States National Seismic Hazard Maps: U.S Geological Survey Open-File Report 2008-1128*.

Power, M., Chiou, B., Abrahamson, N., Bozorgnia, Y., Shantz, T., and Roblee, C. (2008). "An overview of the NGA project." *Earthq Spectra*, 24(1), 3-21.

Radu, A. and Grigoriou, M. (2014). "A comparative study on fragility analyses in earthquake engineering" *9th International Conference on Structural Dynamics*, June 30-July 2, Portugal

Rezaeian, S., and Der Kiureghian, A. (2010). "Simulation of synthetic ground motions for specified earthquake and site characteristics." *Earthq Eng Struct D*, 39(10), 1155-1180.

Scherbaum, F., Cotton, F., and Staedtke, H. (2006). "The estimation of minimum-misfit stochastic models from empirical ground-motion prediction equations." *B Seismol Soc Am*, 96(2), 427-445.

Taflanidis, A. A., Vetter, C., and Dunbar, R. (2013)."Stochastic ground motion modeling: opportunities and challenges for seismic hazard description in probabilistic risk assessment." *11th International Conference on Structural Safety & Reliability*, June 16-20, New York, NY.

USGS. "U.S. Geological Survey: 2008 Interactive Deaggregations." Retrieved December 1, 2014. *URL* http://geohazards.usgs.gov/deaggint/2008